

***J*-averaged behavior of the core polarization through third order for excitations up to $10 \hbar\omega$**

J. Chai* and S. A. Moszkowski

Department of Physics, University of California, Los Angeles, California 90024

(Received 3 November 1978)

The effect of second order *J*-averaged core polarization on shell model matrix elements was examined through $10 \hbar\omega$ for the intermediate state excitations. It was found that for $^{34}\text{Cl}[(\text{Od}_{3/2})^2]$ the present treatment was quite adequate to provide the needed average repulsion in $T=1$ states, while for $^{40}\text{Ca}[(\text{Od}_{3/2}^{-1}\text{Of}_{7/2})]$ the perturbation treatment fell short by about 0.8 MeV. The tensor effect on higher shell intermediate state excitations was also studied and was found to be more marked for $(\text{Od}_{3/2}^{-1}\text{Of}_{7/2})$. Two particularly large third order terms in the perturbation expansion of the effective interactions were also calculated. Their *J*-averaged effects on $(\text{Od}_{3/2})^2$ and $(\text{Od}_{7/2})$ were found to be small and well-behaved. The *J*-averaged tensor effect calculated in third order was found to saturate by about $10 \hbar\omega$.

[NUCLEAR STRUCTURE Excitation spectra core polarization effective interactions.]

I. INTRODUCTION

Since the discovery of core polarization by Bertsch,¹ and the pioneering systematic calculations by Kuo and Brown² some ten years ago, there has been considerable work done on the perturbation expansion of the nuclear effective interaction in terms of the *G* matrix.³ It was found that by adding the core polarization effect ($2\hbar\omega$ excitation) to the first order ("bare") *G* matrix, the energy spectra of individual *J* levels of some nuclei, e.g., ^{18}O , were greatly improved. On the other hand, Schiffer,⁴ Schiffer and True,⁵ and others⁶ working on the *A*-independent semiempirical effective interactions found that a long-ranged repulsion in the $T=1$ states (with respect to $T=0$ states) was needed in order to fit the experimental data. The microscopic theory of *J*-averaged core polarization may shed some light on the origin of this repulsion, and thus to the splitting in energy centroids of $T=1$ and $T=0$.

The perturbation expansion of linked valence effective interaction \hat{v}_{eff} is given by

$$\hat{v}_{\text{eff}} = G + G \frac{Q}{E_0 - H_0} G + G \frac{Q}{E_0 - H_0} G \frac{Q}{E_0 - H_0} G + \dots,$$

where *G* is the Brueckner reaction matrix (*G* matrix) and *Q* is the Pauli exclusion operator that excludes the model (valence) space from the core excitation orbitals, E_0 is the unperturbed single particle energy of the valence state, and H_0 is the unperturbed single particle energy of the intermediate state.

Two kinds of problems of convergence arise immediately: The first was brought up by Vary, Sauer, and Wong,⁷ who summed the intermediate state excitations up to $22\hbar\omega$ for the individual *JT*

states of ^{18}O , and showed that the results were quite different from those including only $2\hbar\omega$ excitation. Recently Sandel *et al.*⁸ recalculated the second order core polarization for $A=18$ ($JT=01$ and 10) on a shifted harmonic oscillator basis, including the excitations up to $10 \hbar\omega$, and with the starting energy correction in the calculation of the *G* matrix and some other refinements. They arrived at similar conclusions regarding the intermediate-sum convergence as the earlier findings of Vary, Sauer, and Wong.⁷

In Sec. II we write down for the sake of completeness the analytic expressions for the *J*-averaged second order core polarization which can be derived by using the Racah algebra for recoupling of angular momenta. Such relations were first derived by Sartoris and Zamick⁹ and used to calculate the *J*-averaged second order core polarization effect for several different interactions, but only for excitations up to $3\hbar\omega$. In this paper we extend the region of excitations and also use what may be a more realistic interaction, the one proposed by Bertsch *et al.*¹⁰

We calculate the second order effect on $^{34}\text{Cl}(\text{Od}_{3/2})^2$ and $^{40}\text{Ca}(\text{Od}_{3/2}^{-1}\text{f}_{7/2})$ with emphasis on the tensor force and the intermediate state convergence. It is natural to ask if the third and higher order terms in the perturbation expansion of effective interactions also contribute significantly to the energy spectra of these nuclei. (See Fig. 1.) This brings up the difficult problem of convergence of \hat{v}_{eff} order by order in terms of the *G* matrix, the second kind of convergence problem mentioned. In our investigation we do not intend to consider terms beyond third order, but instead, we calculate the *J*-averaged effects for two large third order terms which closely resemble the $G_{3\text{ph}}$ dia-

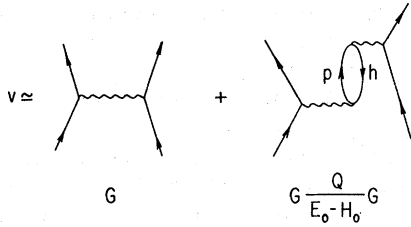
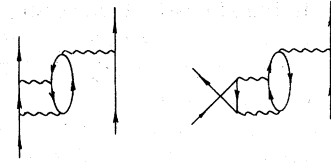


FIG. 1. The diagrammatic representation of the effective interaction used in this calculation.

gram, and examine the higher shell effects in these two third order diagrams.

Barrett and Kirson¹¹ performed the systematical calculations through third order diagrams (and a few fourth order diagrams) with $JT=01$ for intermediate states restricted to $2\hbar\omega$ in energy. They calculated all significant third order terms (15 nonfolded and 4 folded diagrams) and concluded that certain third order $JT=01$ matrix elements were sufficiently large and repulsive so as to nearly cancel the attractive second order $JT=01$ matrix elements. But this cancellation was weakened when Barrett¹² calculated the two largest of the third order ladder terms (Fig. 2) for $JT=01$, and found that they were in general large and attractive, thus reducing the third order repulsion in $JT=01$.

On the other hand, Goode and Koltun¹³ examined the JT average of the perturbation expansion through third order for ^{18}O with excitation no larger than $2\hbar\omega$, and they found that the total third order JT -averaged term was repulsive as



(a) The D-diagram (b) The E-diagram

FIG. 2. The two large third order diagrams used in our calculations.

well as the second order JT -averaged terms, and therefore the conclusion of Barrett and Kirson¹¹ that second and third order terms cancel for $JT=01$ cannot be generalized to other JT states. Goode¹⁴ later calculated all the individual JT states of ^{18}O under the same condition and found that the third order effect on $T=1$ states tends to be small compared to the corresponding second order effect, while for $T=0$ states (tensor part) the third order effect tends to cancel the second order effect. Although second and third order effects in perturbation expansion do not consistently cancel, it was found that in JT average,^{4,5} the core polarization is repulsive in second and third order, at least for ^{18}O .

In our calculation we compute the J -averaged effect of two particular large third order terms,^{11,14} the "vertex renormalization diagrams" (Fig. 2), for $(O_{d_{3/2}})^2$ and $(O_{d_{3/2}}^{-1}O_{f_{7/2}})$, and our emphasis is to see the effect of these two third order terms on the isospin splitting ($T=1-T=0$) in the energy centroids, when including the intermediate-state energies up to $10\hbar\omega$.

II. J -AVERAGED SECOND ORDER CORE POLARIZATION

In order to examine the isospin splitting between $T=1$ and $T=0$ energy centroids for $N=Z$ nuclei in the light of second order core polarization, we have to find a general expression in the J -weighted average for the second order core polarization. This J -independent effect can be understood in terms of Bansal and French's force of the form $V = -a + b\vec{t}_1 \cdot \vec{t}_2$,¹⁵ where a and b are the parameters of the monopole interaction.

The J -averaged second order core polarization (diagonal matrix elements) can then be shown to be^{9,16}

$$\begin{aligned}
 \left\langle j_1 j_2 J T \left| \frac{G_{3p1h}}{E_0 - H_0} \right| j_1 j_2 J T \right\rangle_{\bar{J}} &= - \frac{1}{[(1 + \delta_{ab})(1 + \delta_{cd})]^{1/2}} \frac{1}{(2j_1 + 1)(2j_2 + 1)} W_s \\
 &\times \sum_{\epsilon_h - \epsilon_p} \frac{1}{\epsilon_h - \epsilon_p} \sum \frac{1}{[(2T + 1)(2T'' + 1)]^{1/2}} u(\frac{11}{22} \frac{11}{22}, TT'') \\
 &\times \sum [(2T''' + 1)(2T_4 + 1)]^{1/2} u(\frac{1}{2} \frac{1}{2} \frac{11}{22}, T''' T'') u(\frac{1}{2} \frac{11}{22}, T_4 T''') (2J''' + 1) \\
 &\times \left[G(j_1 h p j_2, J''' T''') G(j_1 h p j_2, J''' T_4) + G(j_2 h p j_1, J''' T''') G(j_2 h p j_1, J''' T_4) \right. \\
 &\left. - 2\delta_{j_h j_p} (-)^{T+j_1+j_2+J'''+J_4} \left(\frac{2J_4 + 1}{2j_h + 1} \right) G(j_1 h p j_1, J''' T''') G(j_2 h p j_2, J_4 T_4) \right], \quad (2.1)
 \end{aligned}$$

where W_S is the statistical weighting factor due to the different orbits: $W_S=1$ for $j_1 \rightarrow Od_{3/2}$ and $j_2 \rightarrow Of_{7/2}$, $W_S=\frac{4}{5}$ for $j_1=j_2 \rightarrow Od_{3/2}$ and $T=0$, and $W_S=\frac{4}{3}$ for $j_1=j_2 \rightarrow Od_{3/2}$ and $T=1$.

Although Eq. (2.1) involves particle-particle matrix elements only, it can be shown^{9,16} that $\langle G_{3ph}(j_1 j_2) \rangle_{\mathcal{J}} = \langle G_{3ph}(j_1^{-1} j_2) \rangle_{\mathcal{J}}$ by applying the Pandya relation. This is useful for the case of $^{40}\text{Ca}[(Od_{3/2}^{-1} Of_{7/2})]$ where for the J -averaged G_{3ph} we can interchangeably use $(Od_{3/2} Of_{7/2})$ in place of $(Od_{3/2}^{-1} Of_{7/2})$.

III. J-AVERAGED ANALYTIC EXPRESSIONS FOR THIRD ORDER DIRECT AND EXCHANGE DIAGRAMS

The analytic expressions for the J average of these two (and other) third order diagrams (Fig. 2) can be obtained by applying the standard diagram rules outlined by Brandow,¹⁷ and Racah algebra

for recoupling of angular momenta.^{16,18} However, these analytic expressions are by no means unique, since the coupling of three or more angular momenta can be chosen in a number of different ways, and this may result in a number of different analytic expressions for each diagram.¹¹ All expressions for each one diagram are equivalent in the sense that each one can be derived from the others by appropriate manipulations of the recoupling coefficients. We choose to write our expressions in terms of Wigner's 6- j symbols or U coefficients (normalized 6- j symbols with appropriate phase relation) since they possess greater symmetry and are easier to manipulate.

The J -averaged process simplifies the expressions by virtue of the sum rules and other relations of the U coefficients, and we have for the D diagram with $a=c+1$ and $b=d+2$ and the shorthand notation $\hat{j} \equiv 2j+1$, $u(TT_1) \equiv u(\frac{1}{2} \frac{1}{2} \frac{1}{2} \frac{1}{2}, TT_1)$

$$\begin{aligned}
\langle D(T) \rangle_{\mathcal{J}} = & -\frac{1}{(1+\delta_{ab})^{1/2}(1+\delta_{cd})^{1/2}} \left(\frac{1}{E_0 - H_0} \right)^2 \left(\frac{1}{\hat{j}_1 \hat{j}_2} \right) W_S \\
& \times \left\{ \delta_{j_x j_v} \sum_{\text{all } J T^s} \frac{(-1)^{j_2+j_x}}{\hat{j}_v} (-1)^{T+J_1} \left(\frac{\hat{j}_1^2 \hat{T}_1}{\hat{T} \hat{T}_2} \right)^{1/2} u(TT_2) u(T_1 T_L) G(v22x, J_1 T_1) \right. \\
& \times \sum (-1)^{T_g} \left(\frac{\hat{j}_2^2 \hat{T}_2 \hat{T}_3}{\hat{T}_g} \right)^{1/2} u(T_2 T_g) u(T_3 T_g) u(T_g T_L) G(xyw1, J_2 T_2) G(vywl, J_2 T_3) \\
& + \delta_{j_x j_v} \sum_{\text{all } J T^s} \frac{(-1)^{j_1+j_x}}{\hat{j}_v} \sum (-1)^{T+J_1} \left(\frac{\hat{j}_1^2 \hat{T}_1}{\hat{T} \hat{T}_L} \right)^{1/2} u(TT_L) u(T_1 T_L) G(v11x, J_1 T_1) \\
& \times \sum (-1)^{T_g} \left(\frac{\hat{j}_2^2 \hat{T}_2 \hat{T}_3}{\hat{T}_g} \right)^{1/2} u(T_2 T_g) u(T_3 T_g) u(T_g T_L) G(xyw2, J_2 T_2) G(vyw2, J_2 T_3) \\
& + \sum (-1)^{j_1+j_x} \sum (-1)^{\epsilon+T_g} (\hat{g} \hat{T}_g \hat{T}_L \hat{T})^{-1/2} u(T_g T_L) u(j_2 j_v j_1 j_x, gL) \\
& \times \sum (\hat{j}_1 \hat{T}_1)^{1/2} u(TT_L) u(T_1 T_L) u(j_2 j_x j_1 j_v, J_1 L) G(v12x, J_1 T_1) \\
& \times \sum (\hat{j}_2 \hat{j}_3 \hat{T}_2 \hat{T}_3)^{1/2} u(T_2 T_g) u(T_3 T_g) u(j_v j_y j_2 j_w, J_2 g) u(j_x j_y j_1 j_w, J_3 g) G(vyw2, J_2 T_2) G(xyw1, J_3 T_3) \\
& + \sum (-1)^{j_2+j_x} \sum (-1)^{\epsilon+T_g} (\hat{g} \hat{T}_g \hat{T}_L \hat{T})^{-1/2} u(T_g T_L) u(j_1 j_v j_2 j_x, gL) \\
& \times \sum (\hat{j}_1 \hat{T}_1)^{1/2} u(TT_L) u(T_1 T_L) u(j_1 j_x j_2 j_v, J_1 L) G(v21x, J_1 T_1) \\
& \times \sum (\hat{j}_2 \hat{j}_3 \hat{T}_2 \hat{T}_3)^{1/2} u(T_2 T_g) u(T_3 T_g) u(j_v j_y j_1 j_w, J_2 g) u(j_x j_y j_2 j_w, J_3 g) G(vyw1, J_2 T_2) G(xywz, J_3 T_3) \left. \right\}, \tag{3.1}
\end{aligned}$$

and for the E diagram

$$\begin{aligned}
\langle E(T) \rangle_{\vec{J}} = & -\frac{1}{(1+\delta_{ab})^{1/2}(1+\delta_{cd})^{1/2}} \left(\frac{1}{E_0 - H_0} \right)^2 \left(\frac{1}{\hat{j}_1 \hat{j}_2} \right) W_S \\
& \times \left\{ \delta_{j_y, j_v} \sum_{\text{all } J T \text{'s}} \frac{(-1)^{j_2 + j_v}}{\hat{j}_v} \sum (-1)^{T+J_1} \left(\frac{\hat{J}_1^2 \hat{T}_1}{\hat{T} \hat{T}_L} \right)^{1/2} u(T T_L) u(T_1 T_L) G(v 2 2 y, J_1 T_1) \right. \\
& \times \sum (-1)^{T_g} \left(\frac{\hat{J}_2^2 \hat{T}_2 \hat{T}_3}{\hat{T}_g} \right)^{1/2} u(T_2 T_g) u(T_3 T_g) u(T_g T_L) G(w y 1 x, J_2 T_2) G(w v 1 x, J_2 T_3) \\
& + \delta_{j_y, j_v} \sum \frac{(-1)^{j_1 + j_v}}{\hat{j}_v} \sum (-1)^{T+J_1} \left(\frac{\hat{J}_1^2 \hat{T}_1}{\hat{T} \hat{T}_L} \right)^{1/2} u(T T_L) u(T_1 T_L) G(v 1 1 y, J_1 T_1) \\
& \times \sum (-1)^{T_g} \left(\frac{\hat{J}_2^2 \hat{T}_2 \hat{T}_3}{\hat{T}_g} \right)^{1/2} u(T_2 T_g) u(T_3 T_g) u(T_g T_L) G(w y 2 x, J_2 T_2) G(w v 2 x, J_2 T_3) \\
& + \sum_{\text{all } J T \text{'s}} (-1)^{j_2 + j_v} \sum (-1)^{\epsilon + T_g} (\hat{g} \hat{T}_g \hat{T}_L \hat{T})^{-1/2} u(T_g T_L) u(j_2 j_v j_1 j_y, g L) \\
& \times \sum (\hat{J}_1 \hat{T}_1)^{1/2} u(T T_L) u(T_1 T_L) u(j_2 j_y j_1 j_v, J_1 L) G(v 1 2 y, J_1 T_1) \\
& \times \sum (\hat{J}_2 \hat{T}_2 \hat{T}_3)^{1/2} u(T_2 T_g) u(T_3 T_g) u(j_y j_w j_1 j_x, J_2 g) u(j_v j_w j_2 j_x, J_3 g) G(w y 1 x, J_2 T_2) G(w v 2 x, J_3 T_3) \\
& + \sum (-1)^{j_1 + j_v} \sum (-1)^{\epsilon + T_g} (\hat{g} \hat{T}_g \hat{T}_L \hat{T})^{-1/2} u(T_g T_L) u(j_1 j_v j_2 j_y, g L) \\
& \times \sum (\hat{J}_1 \hat{T}_1)^{1/2} u(T T_L) u(T_1 T_L) u(j_1 j_y j_2 j_v, J_1 L) G(v 2 1 y, J_1 T_1) \\
& \times \sum (\hat{J}_2 \hat{T}_2 \hat{T}_3)^{1/2} u(T_2 T_g) u(T_3 T_g) u(j_y j_w j_2 j_x, J_2 g) u(j_v j_w j_1 j_x, J_3 g) G(w y 2 x, J_2 T_2) G(w v 1 x, J_3 T_3) \left. \right\}. \tag{3.2}
\end{aligned}$$

IV. NUMERICAL INVESTIGATION OF SECOND ORDER CORE POLARIZATION DIAGRAM

To evaluate the J -averaged second order core polarization $\langle G_{3p1h} \rangle_{\vec{J}}$ we have to decide on the appropriate nuclear force (G) to use, and then generate all the particle-particle matrix elements of that force needed for the evaluation of $\langle G_{3p1h} \rangle_{\vec{J}}$ in Eq. (2.1). For the second order calculation, the U coefficients are very simple—all of the form $U(\frac{1}{2} \frac{1}{2} \frac{1}{2} \frac{1}{2}, T T')$ type.

A. Bertsch force

The force we used for our calculation is a set of effective local interactions derived by fitting the matrix elements of the sum of the Yukawa and/or the regularized one-pion exchange potential (ROPEP) to three selective sets of G -matrix elements of Hamada-Johnston, Reid soft core and Elliott potentials.¹⁰ We will call this force the Bertsch force thereafter. The various components of the Bertsch force we used in the calculation are

TABLE I. Regular Bertsch force.

Channel	Strength (MeV)			
	$R_1 = 0.25$ fm	$R_2 = 0.40$ fm	$R_3 = 1.414$ fm	$R_3' = 0.7$ fm
SE	12 454	-3835	-10 463	...
TE	21 227	-6622	-10 463	...
TO	3.488	...
TNE	...	-1259.6	...	-28.41
TNO	...	283.0	...	13.62
LSE	...	-813.0
LSO	-3733	-427.3
SO	5018	1810

TABLE II. First order (bare) matrix elements in MeV with $\hbar\omega=14$ MeV.

T	J	Ours ^a	$(0d_{3/2})^2$ (KB) ^b	ROPEP ^c	Ours ^a	$(0d_{3/2}0f_{7/2})$ (KB) ^b	ROPEP ^c
0	1	+0.0092	-0.222	-1.255			
	2				-4.305	-3.502	-3.589
	3	-2.8876	-2.435	-3.367	-2.942	-2.294	-2.065
	4				-1.268	-0.956	-1.036
	5				-3.514	-3.095	-3.254
1	0	+0.0504	-0.087	-0.970			
	2	-0.1806	-0.281	-0.385	-0.354	-0.508	+0.071
	3				-0.393	-0.499	-0.547
	4				-0.286	-0.340	+0.017
	5				-1.810	-1.789	-1.783

^aRegular Bertsch.^bP. Goode, private communication.^cBertsch ROPEP for tensor components.

given in Table I.

The two-body shell model matrix element in the H. O. basis that involves the local potential at all is the reduced radial integral (Talmi integral): $\langle nl | v(r_{ij}) | n'l' \rangle$. Owing to the very strong repulsion in short internucleonic distance for realistic forces, the G matrix or a well-fitted force that is assured of finite values and smooth behavior at short distance has to be used. We prepared a computer code that uses the Bertsch force and generates the two-body shell model matrix elements in the H. O. basis. In Table II we compare the bare Bertsch (first order) matrix elements to those of Kuo and Brown for $(0d_{3/2})^2$ and $(0d_{3/2}0f_{7/2})$ with $\hbar\omega=14$ MeV. In Table III we show again the first order Bertsch matrix elements, with the $\hbar\omega$ values appropriate to $A=34$ and $A=40$ for $(0d_{3/2})^2$ and $(0d_{3/2}0f_{7/2})$ respectively, through the

relation $\hbar\omega=41A^{-1/3}$ MeV. The experimentally derived values for $(0d_{3/2})^2$ and $(0d_{3/2}0f_{7/2})$ are also listed for comparison. Immediately noticeable is the large discrepancy between the theoretical first order energy centroid splitting and the experimental splitting, especially for the odd-parity states of ^{40}Ca . Similar discrepancies were also found in some other nuclei, e.g., ^{18}O , ^{42}Sc , etc., confirmed by the semiempirical effective interaction approach of Schiffer and others. The second order core polarization could, from the microscopic point of view, provide some explanation to this splitting.

B. Comparison with experimental data

The second order J -averaged core polarization is carried out in two steps. First, for a certain

TABLE III. First order (bare) matrix elements and experimental values in MeV for ^{34}Cl and ^{40}Ca .

T	J	^{34}Cl			^{40}Ca (odd parity)	
		Ours ^a	Expt (Schiffer, Ref. 4)	$(0d_{3/2})^2$ Vary and Yang ^b	Ours ^a	Expt (de Voigt, Ref. 19)
0	1	-0.2013	-2.223	-0.001		
	2				-4.017	-4.04
	3	-2.6404	-2.720	-2.089	-2.465	-2.25
	4				-1.156	-1.55
	5				-2.965	-1.95
Centroid		-1.9087	-2.571	-1.575	-2.511	-2.23
1	0	-0.1589	-2.870	-0.165		
	2	-0.1868	+0.160	-0.320	-0.275	+0.83
	3				-0.330	+0.54
	4				-0.219	+0.97
	5				-1.518	+0.19
Centroid		-0.1822	-0.345	-0.294	-0.699	+0.59
Splittings ($T=1-T=0$)		+1.727	+2.23	+1.281	+1.813	+2.82

^aRegular Bertsch.^bPhys. Rev. C 15, 1545 (1977).

TABLE IV. Second order energy splittings (MeV) between $T=1$ and $T=0$ states of $(0d_{3/2})^2$ with regular Bertsch force.

$(0d_{3/2})^2$	$\hbar\omega=12.6558$ MeV		Expt data, Ref. 4	
	@ shell	accumulative	of Schiffer for ^{34}Cl	
$2\hbar\omega$	0.434	0.434		
$4\hbar\omega$	0.109	0.543		
$6\hbar\omega$	0.032	0.575		
$8\hbar\omega$	0.010	0.585		
$10\hbar\omega$	0.004	0.589		Vary and Yang ^b
Second order splitting		0.589		VSW, Ref. 7 0.404
First order splitting ^a		1.727		
Sum		2.320	2.23	

^a From Table II.^b Phys. Rev. C 15, 1545 (1977).

major shell excitation, we use our code and appropriate configurations¹⁶ to generate all the two-body matrix elements appearing in Eq. (2.1); then we use the matrix elements generated in the previous step as inputs into another computer code that evaluates $\langle G_{3p1h} \rangle_{\mathcal{T}}$ in Eq. (2.1).

(i) $^{34}\text{Cl}[(0d_{3/2})^2]$. Owing to the restriction of parity conservation, only even- $\hbar\omega$ excitations are allowed for $(0d_{3/2})^2$.

We calculated the J -averaged second order core polarization effects up to $10\hbar\omega$ for $j_1 = j_2 = (0d_{3/2})^2$ with $\hbar\omega = 14$ MeV (for tests, comparison with other calculations, etc.), and $\hbar\omega = 12.6558$ MeV (for comparison with experimental data of ^{34}Cl). The results with $\hbar\omega = 12.6558$ MeV are tabulated in Table IV. The contribution from each major shell excitation is listed separately first and then the accumulative contribution is listed in the next column. The first order energy splitting (without G_{3p1h}) from Table III for $^{34}\text{Cl}[(0d_{3/2})^2]$ is 1.727 MeV, while the second order effect is 0.589 MeV.

The addition of the second order effect would give a total of 2.32 MeV, pushing the $T=1$ energy centroid up with respect to the $T=0$ energy centroid, and coming very close to the experimental splitting of 2.23 MeV.

(ii) $^{40}\text{Ca}[(0d_{3/2})^{-1}(0f_{7/2})]$ (odd-parity states). The main contributions to the second order core polarization for $(0d_{3/2})^2(0f_{7/2})$ come from odd $\hbar\omega$. The even- $\hbar\omega$ excitations are only available to the $\delta_{j_h j_p}$ term in Eq. (2.1), whose contributions are severely cut down further due to the restriction of the $\delta_{j_h j_p}$.

In Table V we show the results calculated with $\hbar\omega = 11.9885$ MeV which is compatible with $A=40$ through the relationship $\hbar\omega = 41A^{-1/3}$ MeV. Also, for comparison the experimentally derived energy splitting for ^{40}Ca negative-parity particle-particle states due to de Voigt¹⁹ is included in the next column. The J -averaged second order core polarization effects for $(0d_{3/2})^2(0f_{7/2})$ up to $10\hbar\omega$ would push the $T=1$ energy centroid up by 0.23 MeV, with

TABLE V. Energy splittings (MeV) between $T=1$ and $T=0$ states with regular Bertsch force for $(0d_{3/2})^2(0f_{7/2})$.

$(0d_{3/2})^2(0f_{7/2})$	$\hbar\omega=11.9885$ MeV		Experimental	
	@ shell	accumulative	value, Ref. 19 de Voigt: ^{40}Ca	Kuo and Brown, Ref. 2
1 and $2\hbar\omega$	0.082	0.082		0.065
3 and $4\hbar\omega$	0.096	0.178		
5 and $6\hbar\omega$	0.037	0.215		
7 and $8\hbar\omega$	0.011	0.226		
9 and $10\hbar\omega$	0.003	0.229		
Second order splitting		0.229		Sartoris and Zamick, Ref. 9 0.27
First order splitting ^a		1.812		
Sum		2.040	2.82	

^a From Table II.

TABLE VI. Tensor effect on second order energy splitting of $(0d_{3/2})^2$ for each major shell excitation up to $10\hbar\omega$ with Bertsch force.

$(0d_{3/2})^2$	Bertsch force ($\hbar\omega=14$ MeV)		KB, Ref. 2
	Regular (MeV)	Without tensor (MeV)	
$2\hbar\omega$	0.469	0.3422	0.267
$4\hbar\omega$	0.116	0.0853	
$6\hbar\omega$	0.033	0.0196	
$8\hbar\omega$	0.011	0.0061	
$10\hbar\omega$	0.004	0.0032	

respect to the $T=0$ centroid. Sartoris and Zamick⁹ gave a corresponding 0.27 MeV for lower shell excitations with the Kallio-Kolltveit force and $\hbar\omega = 10.5$ MeV. Although the correction is in the right direction, it still falls short of making up for the experimental splitting of 2.82 MeV¹⁹—our first and second order calculations for this multiplet only add up to 2.04 MeV. It is noticed that the first major shell excitation (1 and $2\hbar\omega$) contributes only 0.073 MeV to the splitting, compared with 0.469 MeV of the corresponding $2\hbar\omega$ term for the $(0d_{3/2})^2$ multiplet. One of the reasons is that owing to the limited phase space for this excitation, the number of configurations¹⁶ is relatively small.

C. J -averaged tensor effects

In order to investigate the J -averaged tensor effects we also calculated $\langle G_{3p1h} \rangle_J$ with the Bertsch force *minus* the tensor components. The results with $\hbar\omega = 14$ MeV for the Bertsch force with and without tensor components are shown in Table VI for $(0d_{3/2})^2$ and in Table VII for $(0d_{3/2}0f_{7/2})$. They are also plotted in Fig. 3 and Fig. 4, respectively. The general feature is that the energy splitting between $T=1$ and $T=0$ states due to the second order core polarization in the J -average does converge fairly uniformly from $2\hbar\omega$ up to $10\hbar\omega$ for $(0d_{3/2})^2$, and from $4\hbar\omega$ up to $10\hbar\omega$ for $(0d_{3/2}0f_{7/2})$. For $(0d_{3/2})^2$ the tensor contribution to the J -averaged convergence to the higher shells

seems to be quite limited: The splitting without tensors is about 30–50% less than that with tensors, but for the J -averaged tensor components does not seem to contribute significantly to the rate of convergence to higher shells in $(0d_{3/2})^2$. For $(0d_{3/2}0f_{7/2})$ the situation is somewhat different: With the regular Bertsch force we see that the contribution to the energy centroid splitting is at maximum 3 and $4\hbar\omega$ excitation, then starts to decrease slowly and steadily, while with the Bertsch force *minus* the tensor the decrease is faster toward higher shells, as can be seen from the steeper slope of the dashed line in Fig. 4. This suggests that for $(0d_{3/2}0f_{7/2})$ the effective tensor components have more marked effect on the slowing down of convergence of excitations to higher shells, in the J -weighted average.

V. NUMERICAL INVESTIGATION OF THIRD ORDER DIAGRAMS, $(0d_{3/2})^2$ AND $(0d_{3/2}0f_{7/2})$ MULTIPLETS

The numerical investigation was carried out in three stages: First, we picked out all the contributing configurations appearing in Eq. (3.1) and Eq. (3.2) from the possible orbits for x , y , w , and v for different $n\hbar\omega$ excitations. Rules such as parity consideration and triangular inequalities of angular momenta were used to cut down the great number of contributing configurations. The second stage is to calculate the G -matrix elements and U coefficients for the configurations generated in the first stage. For the interaction matrix elements a computer code was written using the Bertsch force¹⁰ (Table I) (which is essentially a sum of Yukawa potentials fitted to some selected set of Reid soft core, Hamada-Johnston, and Elliott matrix elements; the H. O. spacing parameter $\hbar\omega$ is taken to be 14 MeV). For the U coefficients the usual closed expression for the Racah coefficients was used. The final step is to evaluate the expressions in Eq. (3.1) and Eq. (3.2) separately for D and E diagrams, using the G -matrix elements and U coefficients from step 2 as the inputs.

(i) $(0d_{3/2})^2$ multiplets. Owing to the symmetry

TABLE VII. Tensor effect on energy splittings of $(0d_{3/2}0f_{7/2})$ for each major shell excitation ($\hbar\omega=14$ MeV).

$(0d_{3/2}0f_{7/2})$	Regular	Bertsch force Nodeless approx. ^a	Bertsch force without tensor
1 and $2\hbar\omega$	0.0734	0.0901	0.1089
3 and $4\hbar\omega$	0.0993	0.0980	0.1127
5 and $6\hbar\omega$	0.0397	0.0100	0.0403
7 and $8\hbar\omega$	0.0134	...	0.0106
9 and $10\hbar\omega$	0.0067	...	0.0033

^a Only the matrix elements with $n=n'=0$ orbitals are included.

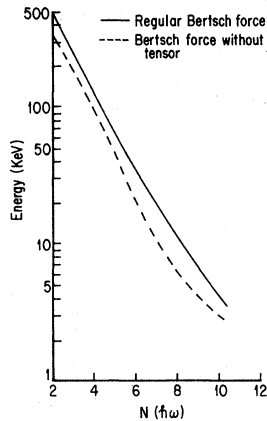


FIG. 3. J -averaged second order core polarization per shell for $(0d_{3/2})^2$ with $\hbar\omega = 14$ MeV.

in this case $a = b = c = d = (0d_{3/2})$, we were able to generate, with limited computing funds, all the interaction matrix elements and U coefficients for the third order calculation up to $10\hbar\omega$ excitations.

The third order results for the J average of D and E diagrams are tabulated in Table VIII. It can be seen that both diagrams have similar contributions to the J -averaged isospin splitting: the small order of magnitude (a few keV) and the apparent intermediate-sum convergence as going up to higher shells. Since the effect of core polarization is negative for low J and repulsive for high J values,¹⁴ this may cause greater cancellation in the J average, resulting in the small J -averaged third order effect. For $(0d_{3/2})^2$ both the second order and the third order J -averaged effects of the core polarization are repulsive, in agreement with the statement made by Goode¹⁴ in his calculation for the sd -shell effective interactions of the mass-18 system. The core polarization through third order seems to be quite adequate to account for the experimental splitting between $T = 1$ and $T = 0$ energy centroids (Table IX).

(ii) $(0d_{3/2}^{-1}0f_{7/2})$ multiplets. Owing to the tremendous number of configurations, we did not calculate the third order effect for the full intermediate

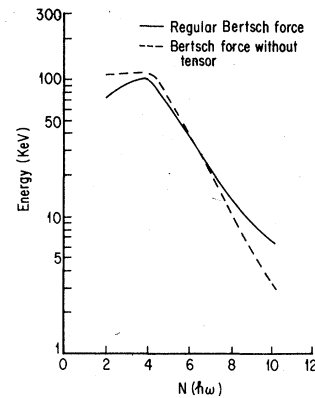


FIG. 4. J -averaged second order core polarization per shell for $(0d_{3/2}0f_{7/2})$ with $\hbar\omega = 14$ MeV.

configurations of each shell excitation up to $10\hbar\omega$ for $(0d_{3/2}^{-1}0f_{7/2})$. Instead, we do the full calculation for the $1\hbar\omega$ and $3\hbar\omega$ excitations for, the D diagram and $1\hbar\omega$ for the E diagram, and then do the same calculations with the nodeless intermediate configurations (a nodeless configuration is one with all four n 's equal to zero) (Table X). A comparison of the results shows that the nodeless configurations in $1\hbar\omega$ excitations contribute more than 90% of the full third order effects in that shell for both D and E diagrams. This is in accordance with the observation made by Kuo and Brown² that the nodeless configurations contribute up to 90% of the total second order core polarization effects in the $2\hbar\omega$ excitation for ^{18}O . Our second order calculation (Table VII) also shows the excellent approximation of the nodeless configurations up to $4\hbar\omega$. Table XI shows the third order J -averaged effects of the nodeless configurations up to $10\hbar\omega$. In the nodeless approximation there seems to be an apparent convergence in the J average when going up to higher shells. The first $2\hbar\omega$ excitation ($D + E$) gives a negative (attractive)¹⁴ contribution, opposite to and about the same order of magnitude of that of second order, and thus seems to cancel the repulsive second order effect, as noted by Barrett^{11,12} and by Goode¹⁴ for $JT = 01$ in the mass-

TABLE VIII. Contributions (MeV) from each major shell excitation to J -averaged third order energy splitting between $T = 1$ and $T = 0$ states of $(0d_{3/2})^2$.

	D diagram	E diagram	$D + E$ diagrams
1 and $2\hbar\omega$	0.007 81	0.006 69	0.014 50
3 and $4\hbar\omega$	0.000 11	0.000 73	0.000 84
5 and $6\hbar\omega$	0.000 10	0.000 08	0.000 18
7 and $8\hbar\omega$	0.000 03	0.000 01	0.000 04
9 and $10\hbar\omega$	0.000 00	0.000 00	0.000 00
Total	0.008 05	0.007 51	0.015 56

TABLE IX. J -averaged effects (MeV) on the isospin energy splitting through third order for $(0d_{3/2})^2$.

First order		Bertsch	Kuo and Brown, Ref. 1	Expt ^a
		1.727	1.52	
Second order	$2\hbar\omega$	0.434	0.267	
	up to $10\hbar\omega$	0.589	...	
Third order	$2\hbar\omega$	0.015	...	
	up to $10\hbar\omega$	0.016	...	
Total	$2\hbar\omega$	2.176	1.787	2.23
	up to $10\hbar\omega$	2.32	...	

^aJ. P. Schiffer, in *The Two-Body Force in Nuclei*, proceedings of a symposium held at Gull Lake, Michigan, 1971, edited by S. M. Austin and G. M. Crawley (Plenum, New York, 1972); J. P. Schiffer and W. W. True, *Rev. Mod. Phys.* **48**, 191 1976.

18 system. From $4\hbar\omega$ and up, the nodeless approximation gives small but positive effects; this somehow reduces the attraction that arises from the $2\hbar\omega$ excitation.

The perturbation calculation of core polarization through third order for pure $(0d_{3/2}^{-1}0f_{7/2})$ does not seem to provide enough $T=1$ and $T=0$ splitting in energy centroids to explain the experimentally derived negative parity states of ^{40}Ca . (Table XII). It is possible that the negative parity states of ^{40}Ca are not entirely populated by the pure $(0d_{3/2}^{-1}0f_{7/2})$ valence configuration, but are mixed with some other valence multilets.

VI. DISCUSSION AND CONCLUSIONS

The first order (bare) shell model matrix elements of the Bertsch forces used in this calculation were found to be comparable to the Kuo-Brown matrix elements, although somewhat more repulsive than the Kuo and Brown's. In our calculation we used the traditional unshifted H. O. single particle wave functions as the basis. Other alternatives have been discussed in the literature,^{3,8} and we will not elaborate them further here.

Our second order J -averaged core polarization results with the Bertsch force agree with previous results of similar calculations.^{2,8} As examples of our formalism we evaluated $\langle G_{3p1h} \rangle_{\bar{J}}$ for ^{34}Cl

and ^{40}Ca . We found that for ^{34}Cl , assuming pure valence $(0d_{3/2})^2$ particle-particle states and $\hbar\omega = 12.6558$ MeV, our J -averaged second order core polarization would give a correction of 0.589 MeV to the first order energy splitting between $T=1$ and $T=0$ states, while for pure $(0d_{3/2}^{-1}0f_{7/2})$ negative-parity states in ^{40}Ca with $\hbar\omega = 11.9884$ MeV the correction is 0.229 MeV. The corrections both give the needed repulsion in the $T=1$ states, and thus explain, at least in part, the origin of this long-ranged repulsion in $T=1$ states found in some (two-valence nucleon) nuclei. We also investigated the numerical importance of intermediate-state excitations to higher shells, and found that, as also pointed out earlier in Ref. 11 for individual J levels of ^{18}O , the higher shell excitations beyond $2\hbar\omega$ should be included in the second order core polarization calculations: For $(0d_{3/2})^2$ our isospin energy splitting increases by 36% from $2\hbar\omega$ to $10\hbar\omega$; for $(0d_{3/2}0f_{7/2})$ the inclusion to $10\hbar\omega$ would increase the splitting by as much as 178%. The contribution from the $2\hbar\omega$ excitation in $(0d_{3/2}0f_{7/2})$ is very small due to the phase space limitation and thus, by comparison, the relative importance of the higher shell excitations is amplified for $(0d_{3/2}0f_{7/2})$.

The second order J -averaged core polarization seems to provide adequate splitting between the $T=1$ and $T=0$ energy centroids for the pure $(0d_{3/2})^2$ states in ^{34}Cl ; but for the pure $(0d_{3/2}^{-1}0f_{7/2})$ in ^{40}Ca , the first and second order

TABLE X. Third order effect for full and nodeless configurations in $(0d_{3/2}0f_{7/2})$.

	D diagram			E diagram		
	Full	Nodeless	%	Full	Nodeless	%
$1\hbar\omega$	-0.047 20	-0.044 66	94.6	-0.047 72	-0.043 09	90.3
$3\hbar\omega$	+0.001 51	+0.001 59	95.0	...	+0.006 44	...

TABLE XI. Nodeless approximation (MeV) for $(0d_{3/2}0f_{7/2})$ to each major shell ($\hbar\omega=14$ MeV).

	D diagram	E diagram	D + E diagrams
1 and $2\hbar\omega$	-0.04457	-0.05163	-0.09620
3 and $4\hbar\omega$	+0.00149	+0.000644	
5 and $6\hbar\omega$	+0.000024	+0.000015	
7 and $8\hbar\omega$	+0.000000	+0.000000	
9 and $10\hbar\omega$	+0.000000	+0.000000	-0.09403

terms provide only some 72% of the total experimental splitting. This may be due to the following reasons: (i) The phase space in the $2\hbar\omega$ excitation for $(0d_{3/2}^{-1}0f_{7/2})$ is very limited. (ii) Some mechanism other than core polarization may be responsible. (iii) Valence configuration mixing in ^{40}Ca (odd-parity states) may be important. (iv) Collective admixtures of nonperturbative nature depress $J^{\pi}T=3^{-}0$ and $5^{-}0$ states.²⁰ Configuration mixing, in general, can be simulated by an effective interaction plus core polarization with a pure valence configuration, as being the case for ^{34}Cl ; but for the odd-parity states of ^{40}Ca , due to the collective admixtures in $J^{\pi}T=3^{-}0$ and $5^{-}0$ states which cause these two states to be considerably depressed in energy, the effective interaction plus the second order core polarization in perturbation treatment is not adequate to explain the splitting in ^{40}Ca .

To investigate the tensor effect on the convergence rate for excitations to higher shells we calculated the J -averaged core polarization contribution from each major shell up to $10\hbar\omega$, with and without tensor components in the Bertsch force. The results were plotted in Figs. 3 and 4. It is noticed that the J -averaged core polarization contribution to higher shells drops smoothly and steadily from $4\hbar\omega$ on, probably due to the facts that in the J -averaged process the fluctuations of

individual J levels are smoothed out, and that the number of contributing configurations in the phase space in higher shells (with increasing energy denominators) is limited. From the graphs we can also see that tensor components seem to play a minor role in the convergence rate for $(0d_{3/2})^2$, while their effects on the convergence rate for $(0d_{3/2}^{-1}0f_{7/2})$ seem quite noticeable. The reason for this behavior is not quite clear to us at this moment. Perhaps it might have something to do with the fact that in the average, for identical orbits as in $(0d_{3/2})^2$, the interaction matrix has fewer and smaller off-diagonal elements, and this means that the tensor is not as operative as for the nonidentical orbit $(0d_{3/2}0f_{7/2})$; therefore for $(0d_{3/2})^2$ the retardation of the drop of the core polarization due to the tensor force is very slight.

Turning to the discussion of third order effects corrections, we have evaluated the J -averaged third order core polarization effect on $(0d_{3/2})^2$ for full intermediate configurations up to $10\hbar\omega$ and find a third order correction of 0.016 MeV which is small and repulsive. Together with the first and second order corrections the core polarization for pure $(0d_{3/2})^2$ would give adequate splitting to explain the experimental isospin $T=1$ and $T=0$ energy centroids of ^{34}Cl . The slight over-repulsive correction can be attributed to the properties of the Bertsch force we chose to use.

TABLE XII. J -averaged effects (MeV) on the isospin energy splitting through third order for $(0d_{3/2}0f_{7/2})$.

First order		Bertsch 1.812	Kuo and Brown, Ref. 2 1.39	Expt ^b
Second order	$2\hbar\omega$	0.082	0.065	
	up to $10\hbar\omega$	0.228	...	
Third order	^a $2\hbar\omega$	-0.096	...	
	up to $10\hbar\omega$	-0.094	...	
Total	$2\hbar\omega$	1.798	1.46	2.82
	up to $10\hbar\omega$	1.947	...	

^a Nodeless configuration contribution only.^b S. de Voigt, private communication (1975); D. Cline *et al.*, Nucl. Phys. **A233**, 91 (1974).

For $(0d_{3/2}^{-1}0f_{7/2})$ multiplets we calculate the J -averaged third order ($D+E$) effects with the full configurations for $1\hbar\omega$ and $3\hbar\omega$ only; for other odd- $\hbar\omega$ excitations only the nodeless approximation is used. For $1\hbar\omega$ excitations we find that the nodeless approximation accounts for more than 90% of the full J -averaged third order effects in the same shell for the D and E diagrams. As we go to higher shell excitations this nodeless approximation is expected to become poorer and poorer because more and more intermediate states are with nodes. However, the nodeless approximation would still give us some idea about the relative strength of the third order effect for the higher shell excitations, although with a decreasing degree of confidence. With the apparent convergence in the higher shells, our nodeless calculation seems to indicate that a negative (attractive) J -averaged third order effect for $(0d_{3/2}^{-1}0f_{7/2})$ is evident. This seems to cancel the second order repulsion and leaves the isospin splitting in the energy centroid of ^{40}Ca (odd-parity states) unexplained, in the light of perturbation treatment of core polarization. This does not, however, invalidate the idea that core polarization is the origin of the long-ranged repulsion in $T=1$ states because of the following possibilities: (1) The odd-parity states of ^{40}Ca may not be made up entirely of pure $(0d_{3/2}^{-1}0f_{7/2})$ valence configuration, and/or (2) the other third order diagrams which are thought to be small and are not included in our calculation may be accumulatively important, and/or (3) there may be some mechanism other than core polarization being operative, in the J average, for the odd-parity states of ^{40}Ca .

A. Configuration mixing

As a result of the strong, interparticle interactions the shell model wave functions are often mixtures of several configurations. In the case of negative-parity states of ^{40}Ca , beside the "original" multiplets $(0d_{3/2}^{-1}0f_{7/2})$, there may be other configurations, for example, $(0d_{5/2}^{-1}0f_{7/2})$, $(1s_{1/2}^{-1}0f_{7/2})$, and $(0d_{3/2}^{-1}1p_{3/2})$, etc., in making up the odd-parity states of ^{40}Ca .

Experimentally the $T=1$, $J^\pi=2^-, 3^-, 4^-$, and 5^- states of ^{40}Ca are very pure $(0d_{3/2}^{-1}0f_{7/2})$ states.²⁰ For $T=0$ states, the situation is not the same: Considerable collective admixtures are believed to be in $J^\pi T=3^-0$ and 5^-0 states.²¹ Therefore the collective admixtures very likely would depress these states significantly in the energy spectrum.

Because the strong interparticle interaction is always present in real nuclei, the physical states observed experimentally are always, more or less, admixtures of some configurations available

to the nucleons in the nucleus. For ^{34}Cl the effect of configuration mixing on the isospin splitting of energy centroids can be mostly "simulated" by the two-body effective interaction plus core polarization of the pure $(0d_{3/2})^2$ configuration. For ^{40}Ca , due to the collective (nonperturbative) admixtures in $J^\pi T=3^-0$ and 5^-0 states, the effective interaction plus core polarization in perturbation treatment for a pure $(0d_{3/2}^{-1}0f_{7/2})$ configuration is inadequate (about 0.9 MeV short) to explain the experimental isospin splitting ($T=1 - T=0$) of energy centroids. A nonperturbative mechanism other than what we dealt with in this investigation may be operative in the negative -parity states of ^{40}Ca , and we will not speculate further here.

B. Nodeless approximation

In the J -averaged second order core polarization calculation we found that nodeless configurations in the lower shell (up to $4\hbar\omega$) contribute up to 80% of the effect of the full intermediate configurations in $(0d_{3/2}^{-1}0f_{7/2})$. The approximation drops to about $\frac{1}{3}$ of the full effect for up to $6\hbar\omega$ excitation, beyond which there is no nonvanishing contributing nodeless configurations.

In the third order calculation for $1\hbar\omega$ and $3\hbar\omega$ excitations the nodeless approximation provides more than 90% of the effect of $(0d_{3/2}^{-1}0f_{7/2})$. After $3\hbar\omega$ we expect the nodeless approximation to drop faster as we go to higher shells, since there are relatively fewer contributing nodeless configurations (about 1 out of 10 configurations is nodeless) in higher shells, making it a less reliable method of approximation for higher shell behavior.

C. Convergence

The contributions from our third order nonfold diagrams ($D+E$) seem to converge in the J average fairly smoothly from the first and second order for $(0d_{3/2})^2$. However, for $(0d_{3/2}^{-1}0f_{7/2})$ the order by order convergence is not as clear-cut. The uncertainty due to nodeless approximation and configuration mixing has to be kept in mind. Although it is difficult to rigorously prove the numerical convergence of the perturbation expansion in powers of the G matrix, there are at least some indications that when appropriate methods of grouping and calculations are used, the series appears to be convergent. Also, the corrections and modifications made by Sandel *et al.*⁸ are suggestive of improved convergence order by order in G , and that previous estimates of the importance of higher order terms in the effective interaction may be too large.

On the other hand, the apparent convergence of

the intermediate sum seems to be observed for $(0d_{3/2})^2$: The J -averaged third order effect drops off by about an order of magnitude when going to the next major shell ($2\hbar\omega$ difference in energy). For $(0d_{3/2}^{-1}0f_{7/2})$ from $3\hbar\omega$ up, our nodeless approximation results also indicate a higher shell convergence. This is in agreement with a recent calculation by Barrett and Goode²² which shows the saturation of tensor effect by $6\hbar\omega$ for some third order diagrams.

From the above results we can see that as far

as the convergence is concerned, both order by order convergence and higher shell convergence, the J -averaged perturbation expansion seems to be better behaved than that of individual J values, at least up to third order. The J -averaged process tends to cancel and smooth out the fluctuations of individual J 's and make the J -averaged core polarization effect generally smoothly small.

This work was supported in part by the National Science Foundation.

*Present address: Cyclotron Laboratory, Michigan State University, East Lansing, Michigan 48824.

¹G. Bertsch, Nucl. Phys. **74**, 234 (1965).

²T. T. S. Kuo and G. Brown, Nucl. Phys. **85**, 40 (1965); **A114**, 241 (1968).

³T. T. S. Kuo, Annu. Rev. Nucl. Sci. **24**, 101 (1974).

⁴J. Schiffer, in *The Two-Body Force in Nuclei*, proceedings of a symposium held at Gull Lake, Michigan, 1971, edited by S. M. Austin and G. M. Crawley (Plenum, New York, 1972).

⁵J. Schiffer and W. True, Rev. Mod. Phys. **48**, 191 (1976).

⁶A. Molinari, M. B. Johnson, H. A. Bethe, and W. M. Alberico, Nucl. Phys. **A239**, 45 (1975); M. Golin and L. Zamick, *ibid.* **A251**, 129 (1975); S. A. Moszkowski, D. Needelman, and M. Golin, Phys. Rev. C **17**, 297 (1978).

⁷J. P. Vary, P. U. Sauer, and C. W. Wong, Phys. Rev. C **7**, 1776 (1973).

⁸M. S. Sandel, R. J. McCarthy, and B. Barrett, Z. Phys. **A280**, 259 (1977).

⁹G. Sartoris and L. Zamick, Phys. Lett. **25B**, 5 (1967).

¹⁰G. Bertsch, J. Borysowicz, H. McManus, and W. G. Love, Nucl. Phys. **A284**, 399 (1977).

¹¹B. Barrett and M. Kirson, Phys. Lett. **27B**, 544 (1968);

30B, 8 (1969); Nucl. Phys. **A148**, 145 (1970).

¹²B. Barrett, Nucl. Phys. **A196**, 638 (1972).

¹³P. Goode and D. S. Koltun, Phys. Lett. **39B**, 159 (1972).

¹⁴P. Goode, Phys. Lett. **51B**, 431 (1974); P. Goode, in *Effective Interactions and Operators in Nuclei (Lecture Notes in Physics)*, edited by B. R. Barrett (Springer, New York, 1975), Vol. 40, p. 151.

¹⁵R. K. Bansal and J. B. French, Phys. Lett. **11**, 145 (1964).

¹⁶J. Chai, Ph.D. dissertation, University of California at Los Angeles, 1977 (unpublished).

¹⁷B. W. Brandow, Rev. Mod. Phys. **39**, 771 (1967).

¹⁸G. Bertsch, *The Practitioner's Shell Model* (North-Holland, Amsterdam, 1972).

¹⁹S. de Voigt, private communication; D. Cline *et al.*, Nucl. Phys. **A233**, 91 (1974).

²⁰R. W. Sharp and L. Zamick, Nucl. Phys. **A208**, 130 (1973).

²¹D. J. Crozier, Nucl. Phys. **A198**, 209 (1972).

²²B. Barrett and P. Goode, in *Proceedings of the International Workshop V on Gross Properties of Nuclei and Nuclear Excitations, Kleinwalsertal, Austria, 1977* [Institution Report No. AED-CONF77-017-001 (unpublished)].